IEEE Access
Multidisciplinary | Rapid Review | Open Access Journal

Received February 9, 2021, accepted March 8, 2021, date of publication March 17, 2021, date of current version March 25, 2021.

Digital Object Identifier 10.1109/ACCESS.2021.3066554

Handover Prediction for Aircraft Dual Connectivity Using Model Predictive Control

SABYASACHI MONDAL, SABA AL-RUBAYE, (Senior Member, IEEE), AND ANTONIOS TSOURDOS, (Member, IEEE)

School of Aerospace, Transport and Manufacturing (SATM), Cranfield University, Cranfield MK430AL, U.K.

Corresponding author: Sabyasachi Mondal (sabyasachi.mondal@cranfield.ac.uk)

This work was supported in part by the Engineering and Physical Sciences Research Council (EPSRC) project CASCADE under Grant EP/R009953/1.

ABSTRACT Providing connectivity to aircraft such as flying taxis is a significant challenge for tomorrow's aviation communication systems. One major problem is to provide ground to air (G2A) connectivity, especially in the airport, rural and sub-rural areas where the number of radio ground stations is not adequate to support the data link resulting in frequent interruption. Hence, effective handover decision-making is necessary to provide uninterrupted services to aircraft while moving from one domain to another. However, the existing handover decision is not efficient enough to solve the aircraft connectivity in such airspace. To overcome this problem, a prediction based optimal solution to handover decision making (handover prediction) would be appropriate to provide seamless dual connectivity to aircraft. In this paper, the handover prediction problem is formulated as a constrained optimization problem in the framework of the model for predictive control (MPC). The cost function and the constraints are derived in terms of dual connectivity variables over the prediction horizon. This problem is solved using a two-dimensional genetic algorithm (2D-GA) to obtain the predictive optimal handover solution. Simulation results show that the proposed dual connectivity handover can significantly improve the handover success probability. Finally, our results show that network densification and predictive control model have improved aircraft performance.

INDEX TERMS Handover, dual connectivity, model predictive control, two-dimensional genetic algorithm (2D-GA).

I. INTRODUCTION

Air transport connectivity design is a key factor to measure the efficiency in competitive aerospace industries. Nowadays, different types of unmanned aircraft are used for applications like aerial surveillance, package delivery, and flying taxis [1]. During the past couple of years, providing real-time data link to access network resources anytime and anywhere has become a big challenge for the aircraft industry. This challenge becomes more difficult for a critical mission like disaster recovery operations, where real-time data needs to be transmitted continuously. The feasibility of long-term evolution (LTE) based aircraft communication is studied through a set of measurements in the field trial to estimate the signal to noise ratio (SNR) for the downlink while assuming free space propagation conditions and ignoring the effect of non-line-of-sight (NLoS) links [2], [3]. Therefore, there is a high demand for seamless radio communications link need to be deployed quickly to enable the flow of data services using air-to-air (A2A) and air-to-ground (A2G) links. With the rapid development of data communications, the International Telecommunication Union (ITU) predicts that the launch of the fifth-generation (5*G*) networks in the near future will play a significant role in the airspace domain and pave ways for novel applications. Using this technology, the aircraft communication systems will reach a speed of 100 GB/s with a data rate capacity of almost 1000 times wider than the existing system. In the case of an aircraft under 5*G*, domain [4], will have less dynamic network segments of the handover architecture that can help to provide seamless connectivity with the core network. It can be mentioned that the handover procedure refers to transferring a connected user's session from a base station to another base station without causing interruption to the session. The system must provide mobility

The associate editor coordinating the review of this manuscript and approving it for publication was Hualong Yu.

This work is licensed under a Creative Commons Attribution 4.0 License. For more information, see https://creativecommons.org/licenses/by/4.0/

to the users reliably without dropping any of their calls / losing their data. The key challenges that technology needs to address are the high coverage and uninterrupted connectivity during the handover process to ensure continuous control and tracking of autonomous or piloted aircraft [5]. It will enhance the provision of data exchange services and real-time streaming between the aircraft and ground station. The requirement of backhauling for seamless dual connectivity, however, remains an inherent challenge to the clarity of aircraft in a 5*G* network [6]. In the case of 5*G*, the handover problem can happen when the radio data link gets damaged and the aircraft wants to transmit the measurement reports while the uplink connectivity is degraded. Therefore the aircraft will not be able to send the reports to the ground network station. The other way around, in some cases, the ground station attempt to respond with a handover command that may never reach the aircraft either because the transmission power of downlink connectivity is not enough or the handover command is too large, which required multiple transmissions.

In the handover decision process, the ground base station continuously monitors each aircraft vehicle's signal strength and reports to the mobility management entity (MME), making the handover decision. In addition to measuring the RSSI (Radio Signal Strength Measurement) of the sessions in progress within the cell, a spare receiver in each base station called a locator receiver is used to scan and determine the aircraft vehicle's signal strength which are in neighbouring cells. The Locator receiver is controlled by the MME, usually used to monitor an aircraft's signal strength in neighbouring cells, which appear to need handover and records all RSSI values to the MME. SNR is the preferred signal parameter measured and monitored and crucial to handover decision-making in such mobility models. If the handover decision at each time interval is possible to predict in advance depending on the signal strength, then it is easier for the ground station to maintain continuous data link connectivity to ensure seamless handover during continuous transmission of control command and data exchange. There are very few relevant works exploring the aircraft connectivity and handover decision [7] in aerospace networking [4], [8], [9], but none of them presented an optimum solution to predict handover. To meet the new aviation capacity requirements for the rapid growth of aircraft data traffic and operations, this paper presents a new mechanism that predicts the optimal aircraft dual handover decision a priori by solving an optimization problem derived in Model Predictive Control (MPC) framework [10]–[12]. MPC is a well-established predictive control theory, including convergence and optimality guarantees for both linear and nonlinear problems under relevant assumptions [13], [14].

Although the concept of dual connectivity for mobile handover has been addressed in 3*GPP* standard, there are still many challenges regarding aircraft/flying tax to achieve seamless motility handover. Particularly when considering a new technology integration with 5*G* backhaul and satellite networks. This integration is considered in 3*GPP* release 17, which is not completed yet. Hence, this work is presented with new techniques to overcome the problem of mobility prediction based optimal solution for handover decision making.

The contribution in this paper is given as follows.

- The novelty of this paper is to model the handover prediction for dual connectivity in MPC framework, which can handle the challenges imposed on the infrastructure of ground access networks. The idea is very new and helpful in understanding the optimal handover of aircraft for long-range operation.
- The future handover decisions of aircraft are predicted in advance such that the handover overhead over the prediction horizon is minimized considering the communication constraints. The solution helps to avoid unnecessary handover for the aircraft. It satisfies the constraints on datalink capacity of LOS and satellite communication.
- The use of bio-inspired algorithm like genetic algorithm is new in this context.

The rest of this paper is organized as follows. The handover mechanism is presented in Section II. In Section III, preliminaries, and the mathematical model of the optimization problem for handover prediction for dual connectivity are presented. The two-dimensional genetic algorithm, i.e., the solution method is presented in Section IV. Simulation results and analysis are given in Section V. Finally, conclusions are drawn.

II. HANDOVER MECHANISM

Handover procedures enable the maintenance of ongoing data link connectivity while an aircraft moves across different base stations networks. When the Aircraft moves between different cells while a conversation is in progress, it automatically transfers the session to a new channel. Handover operation involves identifying a new base station and requires that the data and control signals be allocated to channels with the new base station. Handover must be performed successfully, for this system designer must specify an optimum signal level to initiate a handover. Once a signal level is identified as the minimum usable signal for acceptable voice quality at the base station receiver, a slightly stronger signal level is used as a threshold at which a handover is made.

There are two types of handover, hard and soft. In hard handover, the user disconnects from the source cell before connecting to the target cell. In soft handover, the user connects to the target cell before disconnecting from the source cell. In LTE, only hard handover is supported. The two types of handover are compared in Table 1. In the radio communication system, the terms handover or handoff refer to transferring an ongoing call or data session from one channel connected to another channel's core network. In satellite communications, it is the process of transferring satellite control responsibility from one earth station to another without loss or interruption of service. Fig. 1 depicts the handover scenarios of a flying taxi vehicle involving both radio and satellite communication based on geographical locations.

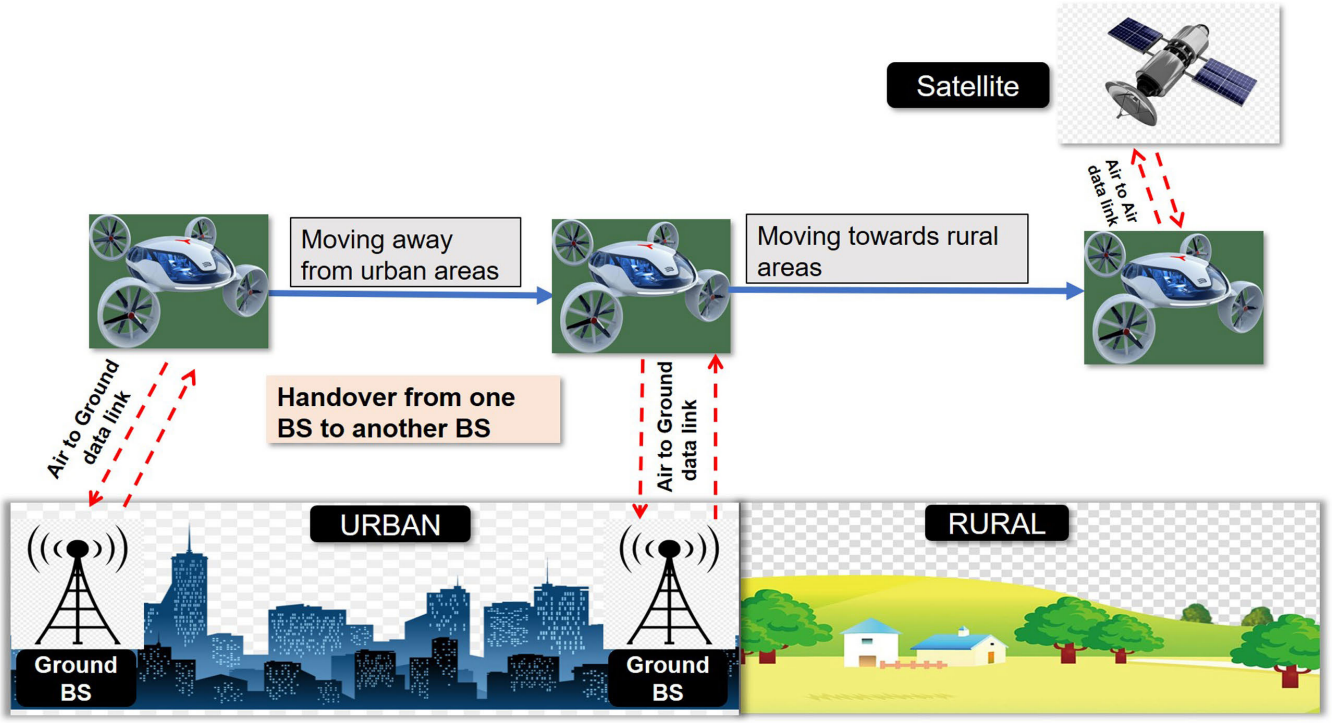


FIGURE 1. Dual connectivity scenario for modern aircraft.

TABLE 1. Comparison between hard and soft handover.

Hard Handover	Soft Handover
1. It uses only one channel at a time	1. It uses multiple channels at a time
2.The event is short and usually unnoticeable	2.It is a status of the service and source channel is broken only when new reliable channel connection is made
3. The UE need not support the use of two channels at the same time	3. Due to the use of multiple channels the probability of a fade or interference in all the channels at the same time is less.
4. Cheaper and Simpler Service maybe disrupted or terminated temporarily	4. Complex hardware in the UE Service is much more reliable due to the parallel use of channels

Urban areas have a higher volume of cell-phone towers as they are required to satisfy the cell phone users. The cell base station users may be supported on the LTE and/or 5*G* network ground stations. These same base station towers can be used to support the aircraft, which will make use of a communications link to communicate with the towers, as shown in Fig. 1.

As the aircraft moves towards the rural area, the signal parameter level falls below the threshold, so the aircraft connectivity will be shifted to a satellite. The source ground base station keeps sending the measurement control signal, which serves the purpose of monitoring the signal to noise ratio (SNR) value, and in turn, the aircraft vehicle sends the measurement reports. The ground base station then, based on the SNR value makes the handover decision. If a handover is needed, then the source ground base station sends a handover request to the target satellite located at a 500 km orbit, from where it sends back an acknowledgement signal. The aircraft vehicle then detaches from the old cell and synchronizes with the satellite and delivers the packets to the target satellite. Finally, a path request signal is sent from the target satellite to the data management entity which returns an acknowledgement signal, and the aircraft connectivity switches to the target satellite. This handover process can be affected by some parameter's surroundings, including signal strength and bandwidth insufficiency, flow stream characteristics, and dynamic change in the network topology. In aeronautical communication, this simultaneous association with both LOS and satellite is mechanized by Dual connectivity (DC), which helps the aircraft be connected with the base station via satellites for the beyond-line-of-sight (BLOS) coverage.

The satellite data link can support BVLOS to operate the aircraft or drones for commercial purposes; this has been identified as having the potential for significant economic, societal and environmental benefits. While LOS data link services are used as backhaul for drone and low attitude aircraft networks, to enhance safety and efficiency for commercial BVLOS operation, it is considered that using satellite data link will bring benefits to fully automated low altitude aircraft system to accelerate the widespread commercial deployment of a flying taxi. Such operations will need to be accommodated in the current national and international controlled

airspace and in uncontrolled airspace currently rarely used for aircraft operations. Hence, the satellite data link services can bring significant capacity and reduced latency for backhaul services to remote communities.

III. HANDOVER PREDICTION FOR DUAL CONNECTIVITY USING MPC: MATHEMATICAL DERIVATION

In this section, the predictive system model for the handover for dual connectivity is obtained in the MPC framework, which leads to a binary quadratic optimization problem. Therefore, before going to subsection D, mathematical details of A) handover for dual connectivity, B) quadratic optimization, and C) MPC are presented as preliminaries.

A. OPTIMIZATION PROBLEM FOR DUAL CONNECTIVITY

The mathematical details of handover analysis for dual connectivity is presented here. The traffic queue backlog of i^{th} aircraft is given in Eq. 3 of [9]. The expression is given as follows.

$$Q_i(t+1) = \left[Q_i(t) - x_i(t)R_{L,i}(t) - y_i(t)R_{S,i}(t)\right]^+ + A_i(t) \tag{1}$$

where $[p]^+ = \max\{p, 0\}, i = 1, 2, \ldots, M$. Total number of aircraft supported in the airspace is M. The transmission rate of LOS datalink $R_{L,i}(t)$ and satellite datalink $R_{S,i}(t)$ are estimated for each aircraft.

The handover overhead for each aircraft i is expressed by Eq. 5 of [9]. This parameter is the measure of robustness of the controller's decision. The expression is given by

$$HO_i(t) = \begin{cases} |x_i(t) - x_i(t-1)| + |y_i(t) - y_i(t-1)|, & t \geq 1 \\ x_i(0) + y_i(0), & t = 0 \end{cases}$$

where $x_i(0) + y_i(0)$ is the initial configuration overhead when $t = 0$. It can be mentioned that there are three different values of $HO_i(t)$ when $t \geq 1$. $HO_i(t) = 0$ signifies the link (single or dual connection) for each aircraft remains unchanged. Conversion from one link to another gives the value $HO_i(t) = 1$. The mutual conversion between the datalinks is denoted by $HO_i(t) = 2$. LOS datalink and satellite datalink can support up to N_L and N_S aircraft respectively. The optimization problem presented in [9] is as follows

$$\min \lim_{t\to\infty} \sup \frac{1}{t} \sum_{\tau=0}^{t-1} E[C(\tau)] \tag{2}$$

$$s.t.\ x_i(t) + y_i(t) \geq 1 \tag{3}$$

$$\sum_{i=1}^{M} x_i(t) \leq N_L \tag{4}$$

$$\sum_{i=1}^{M} y_i(t) \leq N_S \tag{5}$$

$$\lim_{t\to\infty} \sup \frac{1}{t} \sum_{\tau=0}^{t-1} E[C(\tau)] < \infty \tag{6}$$

B. QUADRATIC OPTIMIZATION PROBLEM

Quadratic optimization problem requires a system dynamics, a cost function to be optimized, and the constraints on state and control variables. The generalized discrete system dynamics is written as follows.

$$X(k+1) = AX(k) + BU(k) + d(k),\ k = 1, 2, \ldots, N \tag{7}$$

where $X \in \Re^n$ is state, $U \in \Re^m$ is control, and $d(k) \in \Re^n$ is disturbance. The system matrix is $A \in \Re^{n\times n}$, and input matrix is $B \in \Re^{n\times m}$. The objective function is given by

$$J = \lim_{N\to\infty} \frac{1}{N} E\left[\sum_{k=1}^{N-1} L(X(k), U(k))\right] \tag{8}$$

The cost function is given by

$$L(X(k), U(k)) = \begin{bmatrix} X(k) \\ U(k) \end{bmatrix}^T \begin{bmatrix} Q & S \\ S^T & R \end{bmatrix} \begin{bmatrix} X(k) \\ U(k) \end{bmatrix} \tag{9}$$

where $Q = Q^T \in \Re^{n\times n}$, $S \in \Re^{n\times m}$, $R = R^T \in \Re^{m\times m}$.

$$\begin{bmatrix} Q & S \\ S^T & R \end{bmatrix} \geq 0$$

The state and control constraints are written as follows

$$F_X X(k) + F_U U(k) \leq h,\ k = 1, 2, \ldots, N \tag{10}$$

$F_X \in \Re^{q\times n}$, $F_U \in \Re^{q\times m}$. For the case where the state and control constraints are separable i.e., $S = 0$,

$$F_X X(k) \leq h_X \quad F_U U(k) \leq h_U$$

In addition the individual state and control variables have limits like

$$X_{\min} \leq X \leq X_{\max}, \quad U_{\min} \leq U \leq U_{\max}$$

C. MODEL PREDICTIVE CONTROL

In Model Predictive Control, one optimization problem is solved at each time instant. The prediction horizon is N time instants. The problem is formulated as follows.

$$\min\ L_N(X(k+N)) + \sum_{\tilde{k}=1}^{N-1} L(X(k+\tilde{k}), U(k+\tilde{k})) \tag{11}$$

subject to

$$\begin{aligned} F_N X(k+N) &\leq h(N) \\ F_X X(\tilde{k}) + F_U U(\tilde{k}) &\leq h \\ X(\tilde{k}+1) &= AX(\tilde{k}) + BU(\tilde{k}) + \tilde{d} \\ \tilde{k} &= 1, \ldots, N-1 \end{aligned}$$

The optimization variables are $X(k+1), X(k+2), \ldots, X(k+N)$ and $U(k), U(k+1), \ldots, U(k+N-1)$. It can be mentioned that the future value of d i.e., $d(\tilde{k})$ is assumed to be equal to the past average value $\tilde{d}$. $L_N(X(k+N)) : \Re^n \to \Re$ is the terminal cost function given by

$$L_N(X(k+N)) = X(k+N)^T Q_N X(k+N) \tag{12}$$

$Q_N \geq 0$, and $F_N X(k+N) \leq h(N)$ is the terminal state constraint. The optimization problem is a QP whose solution at time instant k is the optimal values of the the variables $U^*(k), U^*(k+1), \ldots, U^*(k+N-1), X^*(k+1), X^*(k+2), \ldots, X^*(k+N)$. The optimal control value $U^*(k)$ is applied at k to obtain state value at $k+1$, i.e., $X(k+1)$. These state values are used to calculate the control at $k+1$ since the control is a function of state feedback.

The optimization variables can be presented in a compact form

$$Z = [U(k)\, X(k+1)\ \ldots\ U(k+N-1)\, X(k+N)] \quad (13)$$

Therefore the optimization problem can be represented as follows

$$\min\ Z^T H Z$$

subject to

$$PZ \leq \tilde{h}, \quad CZ = b$$

where

$$H = \begin{bmatrix} R & 0 & 0 & \ldots & 0 & 0 & 0 \\ 0 & Q & S & \ldots & 0 & 0 & 0 \\ 0 & S^T & R & \ldots & 0 & 0 & 0 \\ \vdots & \vdots & \vdots & \ddots & \vdots & \vdots & \vdots \\ 0 & 0 & 0 & \ldots & Q & S & 0 \\ 0 & 0 & 0 & \ldots & S^T & R & 0 \\ 0 & 0 & 0 & \ldots & 0 & 0 & Q_N \end{bmatrix}$$

$$P = \begin{bmatrix} F_U & 0 & 0 & \ldots & 0 & 0 & 0 \\ 0 & F_X & F_U & \ldots & 0 & 0 & 0 \\ \vdots & \vdots & \vdots & \ddots & \vdots & \vdots & \vdots \\ 0 & 0 & 0 & \ldots & F_X & F_U & 0 \\ 0 & 0 & 0 & \ldots & 0 & 0 & L_N \end{bmatrix}$$

$$C = \begin{bmatrix} -B & I & 0 & 0 & \ldots & 0 & 0 & 0 \\ 0 & -A & -B & I & \ldots & 0 & 0 & 0 \\ 0 & 0 & 0 & 0 & \ldots & 0 & 0 & 0 \\ \vdots & \vdots & \vdots & \ddots & \vdots & \vdots & \vdots & \\ 0 & 0 & 0 & 0 & \ldots & I & 0 & 0 \\ 0 & 0 & 0 & 0 & \ldots & -A & -B & I \end{bmatrix}$$

$$\tilde{h} = \begin{bmatrix} h - F_X X(k) \\ h \\ \vdots \\ h \\ h(N) \end{bmatrix}$$

$$b = \begin{bmatrix} AX(k) + \tilde{d} \\ \tilde{d} \\ \vdots \\ \tilde{d} \\ \tilde{d} \end{bmatrix}$$

D. DUAL CONNECTIVITY HANDOVER PREDICTION: MPC FRAMEWORK

In this section the handover prediction of Dual connectivity problem is formulated in Model Predictive Control framework. In this paper, we have considered the handover problem which is discussed in [9]. The mathematical details are presented in the following section.

1) PREDICTIVE HANDOVER FOR DUAL CONNECTIVITY: MATHEMATICAL DETAILS

The necessary mathematics for handover prediction problem is derived in MPC framework. The main objective is to extend the handover optimization problem given in Eqs. 2-6 over prediction horizon and finally construct an NLP. The derivation starts with Eq. 3 which is written as follows.

$$\begin{bmatrix} 1 & 1 \end{bmatrix} \begin{bmatrix} x_i(t) \\ y_i(t) \end{bmatrix} \geq 1 \quad (14)$$

Eq. 14 can be written for i^{th} aircraft, $i = 1, 2, \ldots, M$. Similar expressions for all the aircraft can be obtained. They are written collectively in Eq. 15.

$$\begin{bmatrix} 1 & 1 & 0 & 0 & \ldots & 0 & 0 \\ 0 & 0 & 1 & 1 & \ldots & 0 & 0 \\ \vdots & \vdots & \vdots & \vdots & \ddots & \vdots & \vdots \\ 0 & 0 & 0 & 0 & \ldots & 1 & 1 \end{bmatrix} \begin{bmatrix} x_1(t) \\ y_1(t) \\ x_2(t) \\ y_2(t) \\ \vdots \\ x_M(t) \\ y_M(t) \end{bmatrix} \geq \begin{bmatrix} 1 \\ 1 \\ \vdots \\ 1 \end{bmatrix} \quad (15)$$

Eq. 15 is written as

$$D^t U(t) \geq I_M \quad (16)$$

where

$$D^t = \begin{bmatrix} 1 & 1 & 0 & 0 & \ldots & 0 & 0 \\ 0 & 0 & 1 & 1 & \ldots & 0 & 0 \\ \vdots & \vdots & \vdots & \vdots & \ddots & \vdots & \vdots \\ 0 & 0 & 0 & 0 & \ldots & 1 & 1 \end{bmatrix} \quad U(t) = \begin{bmatrix} x_1(t) \\ y_1(t) \\ x_2(t) \\ y_2(t) \\ \vdots \\ x_M(t) \\ y_M(t) \end{bmatrix}$$

$$I_M = \begin{bmatrix} 1 \\ 1 \\ \vdots \\ 1 \end{bmatrix}$$

$D^t \in \Re^{M \times 2M}$, $U(t) \in \Re^{2M \times 1}$, and $I_M \in \Re^{M \times 1}$. $U(t)$ is the control vector at time instant t. The queue backlog or state of i^{th} aircraft at $t+1$, i.e., $Q_i(t+1)$ is obtained by the queue backlog or state equation in Eq. 1. The states at $t+1$ for M aircraft are written in a vector form as

$$Q(t+1) = \begin{bmatrix} Q_1(t+1) \\ Q_2(t+1) \\ \vdots \\ Q_M(t+1) \end{bmatrix} \in \Re^{M \times 1} \quad (17)$$

It can be mentioned that the control $U(t)$ is unknown. Therefore $Q(t+1)$ is also unknown. The unknown control vectors at each time instants of the prediction horizon N are $U(t), U(t+1), U(t+2), \ldots, U(t+N-1)$. Similarly, the queue backlog or states of M aircraft at time instants of the prediction horizon N are $Q(t+1), Q(t+2), \ldots, Q(t+M)$. Therefore, all the unknown state and control variables at time $t, t+1, t+2, \ldots, t+N$ are written in a vector form as

$$Z = [U(t)\ Q(t+1)\ U(t+1)\ Q(t+2)\ \ldots\ U(t+N-1) Q(t+N)] \quad (18)$$

It has been assumed that the initial conditions of the states and other parameters at t for M aircraft, i.e., $Q(t) = [Q_1(t)\ Q_2(t)\ \ldots\ Q_M(t)]^T$, are known. The inequality constraints on control in Eq. 3 for all time instants of the prediction horizon $t, t+1, \ldots, t+N-1$ along with Eq. 16 and 18 can be written as

$$\begin{bmatrix} D^t & 0 & 0 & \ldots & 0 & 0 \\ 0 & 0 & D^{t+1} & \ldots & 0 & 0 \\ \vdots & \vdots & \vdots & \ddots & 0 & 0 \\ 0 & 0 & 0 & \ldots & D^{t+N-1} & 0 \end{bmatrix} \begin{bmatrix} U(t) \\ Q(t+1) \\ U(t+1) \\ Q(t+2) \\ \vdots \\ Q(t+N) \end{bmatrix} \geq \begin{bmatrix} I_M \\ I_M \\ \vdots \\ I_M \end{bmatrix} \quad (19)$$

Eq. 19 can be written as

$$D\,Z \geq I \quad (20)$$

$D \in \Re^{M(N-1)\times 3MN}$, $Z \in \Re^{3MN}$, and $I \in \Re^{M(N-1)\times 1}$. Next, the control constraints in Eq. 4 and 5 need to be written in terms of the unknown variable vector Z. First, the Eq. 4 is considered. Eq. 4 is written as

$$\begin{bmatrix} 1\ 1 \ldots 1 \end{bmatrix} \begin{bmatrix} x_1(t) \\ x_2(t) \\ \vdots \\ x_M(t) \end{bmatrix} \quad (21)$$

It can be observed that Eq. 21 consists of control variable x for all aircraft. But control vector $U(t)$ consists of control variables x and y. Therefore Eq. 21 is modified to represent it in terms of $U(t)$ as follows

$$\begin{bmatrix} 1\ 0\ 1\ 0 \ldots 1\ 0 \end{bmatrix} \begin{bmatrix} x_1(t) \\ y_1(t) \\ x_2(t) \\ y_2(t) \\ \vdots \\ x_M(t) \\ y_M(t) \end{bmatrix} \leq N_L \quad (22)$$

Eq. 22 is written as

$$C_x^t\ U(t) \leq N_L \quad (23)$$

where

$$C_x^t = \begin{bmatrix} 1\ 0\ 1\ 0 \ldots 1\ 0 \end{bmatrix} \in \Re^{1\times 2M}$$

Eq. 23 must be written in terms of vector of unknown variable Z. The equation is shown as follows

$$C_x\ Z \leq N_{L_x} \quad (24)$$

where

$$\begin{bmatrix} C_x^t & \mathbf{0} & \mathbf{0} & \mathbf{0} \ldots & \mathbf{0} & \mathbf{0} \\ \mathbf{0} & \mathbf{0} & C_x^{t+1} & \mathbf{0} \ldots & \mathbf{0} & \mathbf{0} \\ \vdots & \vdots & \vdots & \vdots \ddots & \vdots & \vdots \\ \mathbf{0} & \mathbf{0} & \mathbf{0} & \mathbf{0} \ldots & C_x^{t+N+1} & \mathbf{0} \end{bmatrix} \in \Re^{(N-1)\times 3MN}$$

and

$$\mathbf{0} \in \Re^{1\times M}$$
$$N_{L_x} = \begin{bmatrix} N_L\ N_L\ \ldots\ N_L \end{bmatrix}^T \in \Re^{(N-1)\times 1}$$

Similar expression can be obtained for the control variable y

$$\begin{bmatrix} 0\ 1\ 0\ 1 \ldots 0\ 1 \end{bmatrix} \begin{bmatrix} x_1(t) \\ y_1(t) \\ x_2(t) \\ y_2(t) \\ \vdots \\ x_M(t) \\ y_M(t) \end{bmatrix} \leq N_S \quad (25)$$

Eq. 25 is written as

$$C_y^t\ U(t) \leq N_S \quad (26)$$

where

$$C_y^t = \begin{bmatrix} 0\ 1\ 0\ 1 \ldots 0\ 1 \end{bmatrix} \in \Re^{1\times 2M}$$

Also, in terms of unknown vector Z

$$C_y\ Z \leq N_{S_y} \quad (27)$$

where

$$\begin{bmatrix} C_y^t & \mathbf{0} & \mathbf{0} & \mathbf{0} \ldots & \mathbf{0} & \mathbf{0} \\ \mathbf{0} & \mathbf{0} & C_y^{t+1} & \mathbf{0} \ldots & \mathbf{0} & \mathbf{0} \\ \vdots & \vdots & \vdots & \vdots \ddots & \vdots & \vdots \\ \mathbf{0} & \mathbf{0} & \mathbf{0} & \mathbf{0} \ldots & C_y^{t+N+1} & \mathbf{0} \end{bmatrix} \in \Re^{(N-1)\times 3MN}$$

and

$$N_{S_y} = \begin{bmatrix} N_S\ N_S\ \ldots\ N_S \end{bmatrix}^T \in \Re^{(N-1)\times 1}$$

Eq. 24 and 27 are written together as follows

$$C\ Z \leq N \quad (28)$$

where

$$C = \begin{bmatrix} C_x \\ C_y \end{bmatrix} \quad N = \begin{bmatrix} N_{L_z} \\ N_{L_y} \end{bmatrix}$$

Next, the equality constraints are considered. The equality constraints are the queue backlog equation given in Eq. 1. This equation is written as

$$Q_i(t+1) = \left[Q_i(t) - x_i(t)R_{L,i}(t) - y_i(t)R_{S,i}(t)\right]^+ + A_i(t) \quad (29)$$

where $[p]^+ = \max\{p, 0\}$. It can be mentioned that the effect of control variables x_i and y_i are visible in state equation

$$Q_i(t+1) = \left[Q_i(t) - x_i(t)R_{L,i}(t) - y_i(t)R_{S,i}(t)\right] + A_i(t) \tag{30}$$

Therefore the dynamics in Eq. 30 is selected as propagation model to compute the unknown control and state variables Z. The parameters $R_{L,i}(t)$, $R_{S,i}(t)$, and $A_i(t)$ are known at time instant t, but they are unknown for future time instants up to prediction horizon i.e., $t+1, t+2, \ldots, t+N$. In that case, the dynamics is propagated considering average values of these variables. The average values may be obtained using the past values at $\ldots, t-1, t$ of these variables. r_{i_1}, r_{i_2}, and $\tilde{a}$ are assumed the average values of $R_{L,i}(t)$, $R_{S,i}(t)$, and $A_i(t)$ respectively. Therefore Eq. 30 for i^{th} aircraft is written as

$$Q_i(t+1) = \left[Q_i(t) - r_{i_1}x_i(t) - r_{i_2}y_i(t)\right] + \tilde{a} \tag{31}$$

This equation is further simplified as

$$Q_i(t+1) = AQ_i(t) + B_i\begin{bmatrix} x_i(t) \\ y_i(t) \end{bmatrix} + \tilde{a} \tag{32}$$

where $A = 1$ is the scalar system matrix. The input matrix is given by

$$B_i = \begin{bmatrix} -r_{i_1} & 0 \\ 0 & -r_{i_2} \end{bmatrix}$$

Eq. 32 is rearranged to obtain

$$-B_i\begin{bmatrix} x_i(t) \\ y_i(t) \end{bmatrix} + Q_i(t+1) = AQ_i(t) + \tilde{a} \tag{33}$$

Eq. 33 is written for aircraft $i = 1, 2, \ldots, M$ as follows

$$-B^t U(t) + \mathbf{1}_M Q(t+1) = A^t Q(t) + a \tag{34}$$

where

$$B^t = -\begin{bmatrix} B_1 & \mathbf{0} & \ldots & \mathbf{0} \\ \mathbf{0} & B_2 & \ldots & \mathbf{0} \\ \vdots & \vdots & \ddots & \vdots \\ \mathbf{0} & \mathbf{0} & \ldots & B_M \end{bmatrix}$$

$$\mathbf{1}_M = \begin{bmatrix} 1 & 0 & 0 & \ldots & 0 \\ 0 & 1 & 0 & \ldots & 0 \\ \vdots & \vdots & \vdots & \ddots & \vdots \\ 0 & 0 & 0 & \ldots & 1 \end{bmatrix}$$

$$Q(t+1) = \begin{bmatrix} Q_1(t+1) \\ Q_2(t+1) \\ \vdots \\ Q_M(t+1) \end{bmatrix}$$

$$A^t = \begin{bmatrix} A & 0 & \ldots & 0 \\ 0 & A & \ldots & 0 \\ \vdots & \vdots & \ddots & \vdots \\ 0 & 0 & \ldots & A \end{bmatrix}$$

$$Q(t) = \left[Q_1(t)\ Q_2(t)\ \ldots\ Q_M(t)\right]^T$$

$$a = \left[\tilde{a}\ \tilde{a}\ \ldots\ \tilde{a}\right]^T$$

Eq. 34 is written for $t+1, t+2, \ldots, t+N$ as follows

$$P\,Z = R \tag{35}$$

where

$$P = \begin{bmatrix} -B^t & \mathbf{1}_M & \mathbf{0} & \mathbf{0} & \ldots & \mathbf{0} & \mathbf{0} & \mathbf{0} \\ \mathbf{0} & -A^{t+1} & -B^{t+1} & \mathbf{1}_M & \ldots & \mathbf{0} & \mathbf{0} & \mathbf{0} \\ \vdots & \vdots & \vdots & \vdots & \ddots & \vdots & \vdots & \vdots \\ \mathbf{0} & \mathbf{0} & \mathbf{0} & \mathbf{0} & \ldots & -A^s & -B^s & \mathbf{1}_M \end{bmatrix}$$

$$s = t + N - 1$$

and

$$R = \left[A^t Q(t) + a\ a\ a\ \ldots\ a\right]^T$$

The cost function needs to be written in terms of Z. For this, we need to start with the handover expression given by

$$HO_i(t) = |x_i(t) - x_i(t-1)| + |y_i(t) - y_i(t-1)| \tag{36}$$

Similar expression is written for $t+1$

$$HO_i(t+1) = |x_i(t+1) - x_i(t)| + |y_i(t+1) - y_i(t)| \tag{37}$$

The first part of RHS of Eq. 37 is $|x_i(t+1) - x_i(t)|$ which can be written for $i = 1$ as follows

$$|x_1(t+1) - x_1(t)| = \left|\begin{bmatrix} e^t_{x_1} & e^{t+1}_{x_1} \end{bmatrix}\begin{bmatrix} U(t) \\ U(t+1) \end{bmatrix}\right| \tag{38}$$

where

$$e^t_{x_1} = \left[-1\ 0\ \ldots\ 0\right] \in \Re^{1\times 2M}$$
$$e^{t+1}_{x_1} = \left[1\ 0\ \ldots\ 0\right] \in \Re^{1\times 2M}$$

Therefore, the handover overhead for $i = 1$ is written as

$$HO_1(t+1) = \left|\begin{bmatrix} e^t_{x_1} & e^{t+1}_{x_1} \end{bmatrix}\begin{bmatrix} U(t) \\ U(t+1) \end{bmatrix}\right| + \left|\begin{bmatrix} e^t_{y_1} & e^{t+1}_{y_1} \end{bmatrix}\begin{bmatrix} U(t) \\ U(t+1) \end{bmatrix}\right| \tag{39}$$

Eq. 39 is written in terms of Z

$$HO_1(t+1) = \left|E^{t+1}_{x_1} Z\right| + \left|E^{t+1}_{y_1} Z\right| \tag{40}$$

where

$$E^{t+1}_{x_1} = \left[e^t_{x_1}\ \mathbf{0}\ e^{t+1}_{x_1}\ \mathbf{0}\ \ldots\ \mathbf{0}\right]$$
$$E^{t+1}_{y_1} = \left[e^t_{y_1}\ \mathbf{0}\ e^{t+1}_{y_1}\ \ldots\ \mathbf{0}\right]$$

For $i = 2$, the expression of HO is given by

$$HO_2(t+1) = \left|\begin{bmatrix} e^t_{x_2} & e^{t+1}_{x_2} \end{bmatrix}\begin{bmatrix} U(t) \\ U(t+1) \end{bmatrix}\right| + \left|\begin{bmatrix} e^t_{y_2} & e^{t+1}_{y_2} \end{bmatrix}\begin{bmatrix} U(t) \\ U(t+1) \end{bmatrix}\right| \tag{41}$$

where

$$e^t_{x_2} = \left[0\ 0\ -1\ 0\ \ldots\ 0\right]$$
$$e^{t+1}_{x_2} = \left[0\ 0\ 1\ 0\ \ldots\ 0\right]$$

Therefore

$$HO_2(t+1) = \left|E_{x_2}^{t+1} Z\right| + \left|E_{y_2}^{t+1} Z\right| \tag{42}$$

where

$$E_{x_2}^{t+1} = \left[e_{x_2}^{t} \ \mathbf{0} \ e_{x_2}^{t+1} \ \mathbf{0} \ \ldots \ \mathbf{0}\right]$$
$$E_{y_2}^{t+1} = \left[e_{y_2}^{t} \ \mathbf{0} \ e_{y_2}^{t+1} \ \ldots \ \mathbf{0}\right]$$

Similarly, the HO for i^{th} aircraft is given by

$$HO_i(t+1) = \left|E_{x_i}^{t+1} Z\right| + \left|E_{y_i}^{t+1} Z\right| \tag{43}$$

The HO_i for any time instant is given by

$$HO_i(\tau) = \left|E_{x_i}^{\tau} Z\right| + \left|E_{y_i}^{\tau} Z\right|, \quad \tau = t+1, \ldots, t+N \tag{44}$$

It can be observed that each term of RHS of Eq. 44 gives positive value (since they are absolute). Minimization of these terms are equivalent to minimization of their quadratic form. Therefore the cost function can be written as

$$J_i(\tau) = Z^T {E_{x_i}^{\tau}}^T E_{x_i}^{\tau} Z + Z^T {E_{y_i}^{\tau}}^T E_{y_i}^{\tau} Z \tag{45}$$

Eq. 45 is simplified as follows

$$J_i(\tau) = Z^T E_i^{\tau} Z \tag{46}$$

where

$$E_i^{\tau} = {E_{x_i}^{\tau}}^T E_{x_i}^{\tau} + {E_{y_i}^{\tau}}^T E_{y_i}^{\tau}$$

Finally the cost function is written as

$$J = \sum_{i=1}^{M} \sum_{\tau=t+1}^{t+N-1} Z^T E_i^{\tau} Z \tag{47}$$

The optimization problem of Handover in dual connectivity is obtained by combining Eq. 20, 28, 35, and 47

$$\min J = \sum_{i=1}^{M} \sum_{\tau=t+1}^{t+N-1} Z^T E_i^{\tau} Z \tag{48}$$

$$\begin{bmatrix} C \\ -D \end{bmatrix} Z \leq \begin{bmatrix} N \\ I \end{bmatrix} \tag{49}$$

$$P\,Z = R \tag{50}$$

IV. SOLUTION METHOD

The optimization problem given in Eqs. (48-50) is solved using two-dimensional genetic algorithm (2D-GA). A brief discussion about 2D-GA is given in the following section.

A. TWO-DIMENSIONAL GENETIC ALGORITHM (2D-GA)

Two dimensional GA has been used to solve various problems. It is used in packing problem [15] which aims to obtain high packing density. 2D GA is used for flight scheduling problem in [16] where the problem of scheduling of aircraft is solved using 2D GA. The time table or schedule is considered as a 2D chromosome. Also, it is used to obtain optimal communication topology for consensus in [17], [18].

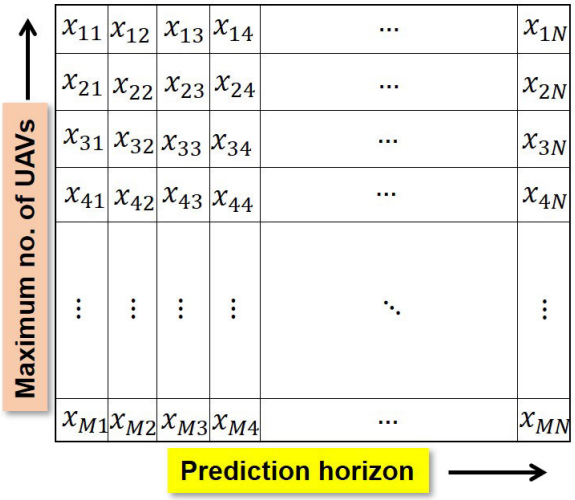


FIGURE 2. Control X over prediction horizon.

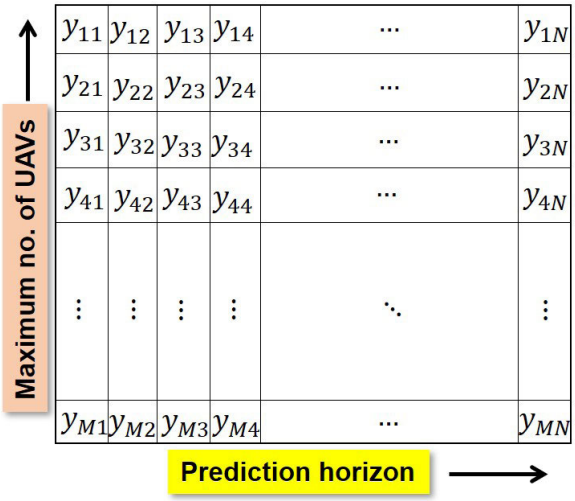


FIGURE 3. Control Y over prediction horizon.

1) TWO-DIMENSIONAL CHROMOSOME REPRESENTATION

The control variables of i^{th} aircraft are given by x_i and y_i. For prediction horizon of length N, the control variables of i^{th} aircraft are written as $x_{ij}, y_{ij}, \ \forall j = 1, 2, \ldots, N$. The control variables for all the agents over prediction horizon are given by $X = [x_{ij}], \ Y = [y_{ij}]; \ \forall i = 1, 2, \ldots, M; \ j = 1, 2, \ldots, N$. Therefore, $X, Y \in \Re^{M \times N}$. They are shown in Figs. 2 and 3 respectively. The 2D chromosome is constructed by combining X and Y and therefore the dimension of each chromosome is $2M \times N$. An example of chromosome is shown in Fig. 4. The elements of the chromosome matrix is denoted by u_{ij} and given in Eq. 51.

$$u_{ij} = \begin{bmatrix} x_{ij} \\ y_{ij} \end{bmatrix} \tag{51}$$

2) POPULATION GENERATION

According to the problem, control variables x_{ij} and y_{ij} can have binary values. N_P is the population size. The population U is generated by Algorithm 1.

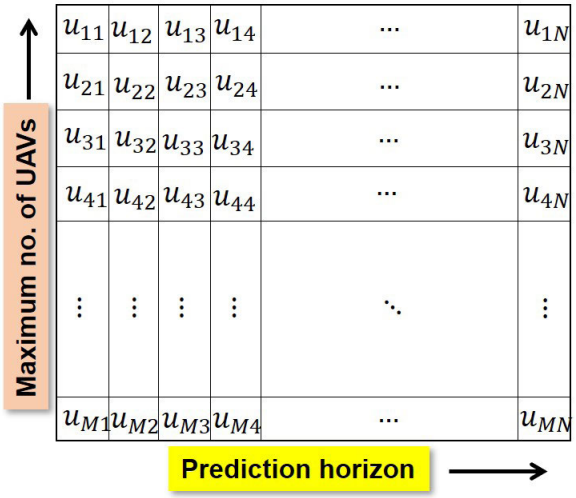


FIGURE 4. 2D chromosome U.

Algorithm 1 Initial Population Generation

```
for l = 1 to N_P do
  for i = 1 to M do
    for j = 1 to N do
      r_x ← random value r_x ∈ (0, 1)
      if r_x > 0.5 then
        x(j) ← 1
      else
        x(j) ← 0
      end if
      r_y ← random value r_y ∈ (0, 1)
      if y_r > 0.5 then
        y(j) ← 1
      else
        y(j) ← 0
      end if
    end for
    u(2i − 1, :) ← x
    u(2i, :) ← y
  end for
  U(:, :, l) ← u
end for
```

In the algorithm, the genes of the chromosomes are created in a random manner. The genes at position (i, j) of the chromosome is selected depending on a random variable $r_x, r_y \in (0, 1)$. N_P chromosomes are collected together to obtain the population U.

3) CROSSOVER

There are a few crossover methods exist in the literature. Some of these methods are Multipoint Crossover [19], Uniform Crossover [20], One-Point Crossover [21], Substring Crossover [21]. More crossover methods can be found in [22].

Crossover method mentioned in [16], is adopted in this work. These methods are presented in algorithmic form. The

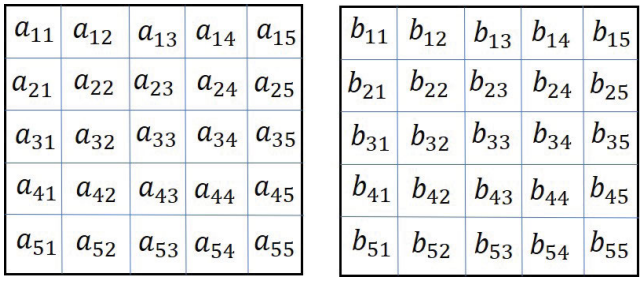


FIGURE 5. Parent Chromosomes.

2D parent chromosomes are denoted by 'Parent 1', and 'Parent 2'. They are shown in Fig. 5. The produced children are denoted by 'Child 1' and 'Child 2'.

Algorithm 2 Substring Crossover

```
r_1 ← random integer < R
r_2 ← random integer < Q
x ← random number x ∈ (0, 1)
if x > 0.5 then
  Execute Horizontal_Crossover(r_1, r_2)
else
  Execute Vertical_Crossover(r_1, r_2)
end if
```

The crossover point is selected in a random manner. Two random integers (r_1 and r_2) are generated, which are less than the maximum number of rows (R) and columns (Q) (R and Q are considered for general representation) of the chromosome as given in Algorithm 2. An example of parent chromosomes is shown in Fig. 5. The genes of Parent 1 is represented by a_{11} to a_{55}. Similarly, the genes of Parent 2 are represented by b_{11} to b_{55}. The crossover point is the gene at position (r_1, r_2) of parent chromosome matrices. The algorithm is explained with the help of an example. In this example, the dimension of parent chromosome matrices is 5×5, i.e., $R = 5$, and $Q = 5$. The crossover position is obtained as $r_1 = 4$, $r_2 = 3$. Therefore the points of crossover for Parent 1 and Parent 2 are a_{43}, and b_{43}, respectively. Next, the type of crossover needs to be selected. For this purpose, a random variable x is considered, which can take any value between 0 and 1. As described in the algorithm, if the value of x is greater than 0.5, the horizontal crossover is selected. Otherwise, for $x < 0.5$, the vertical crossover is chosen. The horizontal crossover function *Horizontal_Crossover*() is described as follows. The rows or part of rows are exchanged between the parents.

The pictorial representation of Algorithm 3 is given in Fig. 6. According to the algorithm, the selected genes of Parent 1, i.e., a_{43} to a_{55} (shown in the red box) are replaced by selected genes of Parent 2, i.e., b_{43} to b_{55} (shown in the blue box) to obtain Child 1. Similarly, a_{43} to a_{55} of Parent 1 is copied in place of b_{43} to b_{55} of Parent 2 to obtain Child 2. In this algorithm, a_{43} and a_{45} of Parent 1 are denoted by $Block1_{P1}$. The genes a_{51} to a_{55} are denoted as $Block2_{P1}$.

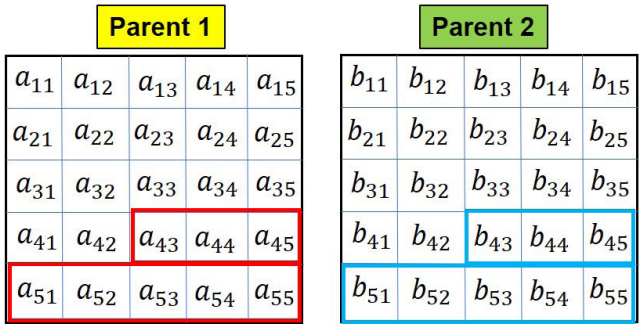


FIGURE 6. Horizontal Crossover: The selected elements of Parent 1 and Parent 2 are shown in green and blue colour respectively.

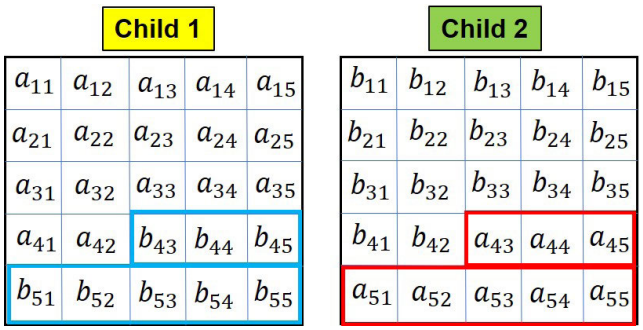


FIGURE 7. Horizontal Crossover: The selected elements of Parent 1 and Parent 2 are exchanged to obtain Child 1 and 2.

Similar elements of the Parent 2 are denoted as $Block1_{P2}$ and $Block2_{P2}$. The Child 1 and 2 are shown in Fig. 7.

Algorithm 3 Function *Horizontal_Crossover*

$Block1_{P1} \leftarrow Parent1(r_1, r_2 : Q)$
$Block2_{P1} \leftarrow Parent1(r_1 + 1 : R, 1 : Q)$
$Block1_{P2} \leftarrow Parent2(r_1, r_2 : Q)$
$Block2_{P2} \leftarrow Parent2(r_1 + 1 : R, 1 : Q)$
$Block1_{P1} \rightleftharpoons Block1_{P2}$ and $Block2_{P1} \rightleftharpoons Block2_{P2}$

The Vertical Crossover algorithm is given in Algorithm 4.

Algorithm 4 Function *Vertical_Crossover*

$Block1_{P1} \leftarrow Parent1(r_1 : R, r_2)$
$Block2_{P1} \leftarrow Parent1(1 : R, r_2 + 1 : Q)$
$Block1_{P2} \leftarrow Parent2(r_1 : R, r_2)$
$Block2_{P2} \leftarrow Parent2(1 : R, r_2 + 1 : Q)$
$Block1_{P1} \rightleftharpoons Block1_{P2}$ and $Block2_{P1} \rightleftharpoons Block2_{P2}$

Vertical crossover is shown in Fig. 8. In this case, selected genes of Parent 1, i.e., a_{43} to a_{55} (shown in the red box) and Parent 2, i.e., b_{43} to b_{55} (shown in the blue box) are exchanged to obtain Child 1 and 2. In the algorithm, a_{43} to a_{53} of Parent 1 are denoted by $Block1_{P1}$. The genes a_{14} to b_{55} are denoted as $Block2_{P1}$. Similar elements of the Parent 2 are denoted as $Block1_{P2}$ and $Block2_{P2}$. The Child 1 and 2 are shown in Fig. 9.

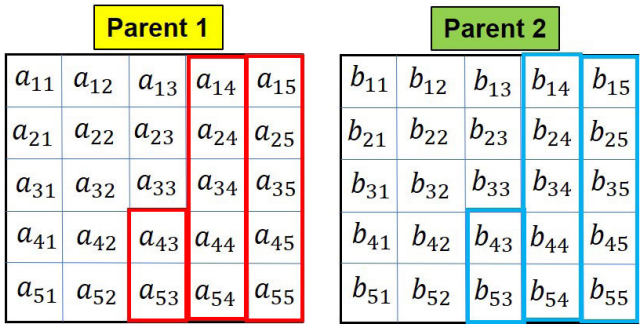


FIGURE 8. Vertical Crossover: The selected columns and part of columns of Parent 1 and Parent 2 are exchanged.

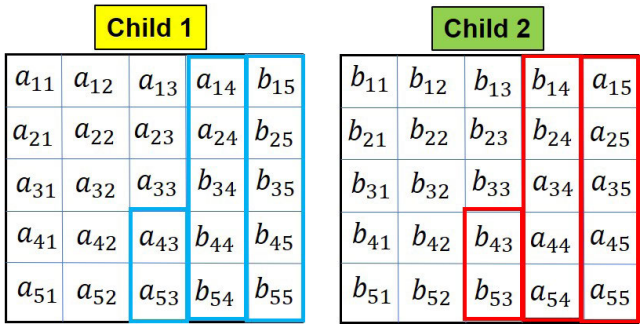


FIGURE 9. Vertical Crossover: The selected columns and part of columns of Parent 1 and Parent 2 are exchanged to obtain Child 1 and 2.

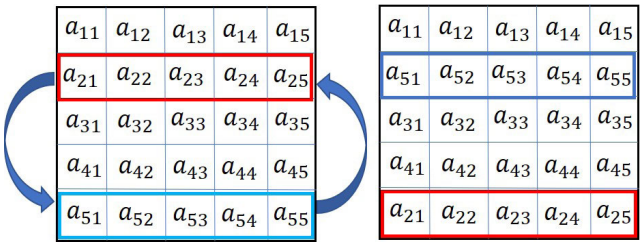


FIGURE 10. Horizontal Swapping: The selected rows are shown in red and blue box. They are swapped.

4) MUTATION

The Mutation is an important operation to preserve the genetic diversity of a population of chromosomes in every generation. The Mutation is performed by exchanging one or more genes of the chromosomes. Generally, a certain percentage of the population is allowed to undergo mutation. The Mutation may change the solution considerably from the previous solution. Hence GA can come to a better solution by using mutation. Few mutation operations are shown in the following algorithms. The process for this mutation is given in Algorithm 5.

The selection of the mutation type is purely random. It depends on a random variable $x \in (0, 1)$. If the value of x is greater than 0.5, then Horizontal Swap function, i.e., *Horizontal_Swap*() is executed. Otherwise, *Vertical_Swap*() is executed.

Horizontal_Swap() function is given in Algorithm 6. It swaps m_1^{th} and m_2^{th} rows of a chromosome. The pictorial representation of the operation is given in Fig. 10. Let us

Algorithm 5 String Swapping Mutation

$x \leftarrow$ random number $x \in (0, 1)$
if $x > 0.5$ **then**
  Execute *Horizontal_Swap*()
else
  Execute *Vertical_Swap*()
end if

Algorithm 6 *Horizontal_Swap*()

$m_1 \leftarrow$ random integer $< R$
$m_2 \leftarrow$ random integer $< R$
if $m_1 \neq m_2$ **then**
  Swap m_1^{th} and m_2^{th} rows of C_k
end if

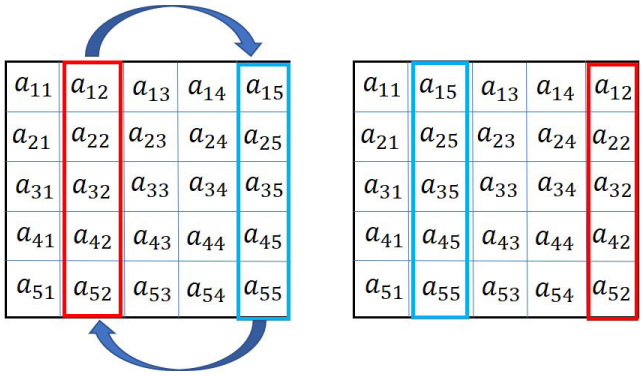


FIGURE 11. Vertical Swapping: The selected columns are shown in red and blue box. They are swapped.

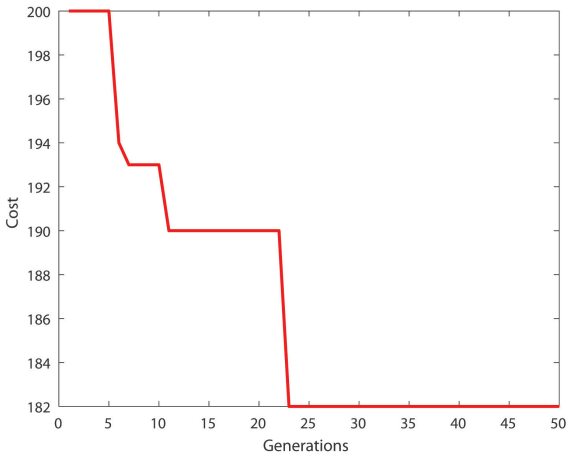


FIGURE 12. Cost produced by 2D-GA.

consider, $m_1 = 1$, and $m_2 = 3$. Therefore, the first and third rows are swapped, as shown in the figure.

Vertical_Swap() function is given in Algorithm 7. It swaps m_1^{th} and m_2^{th} columns of a chromosome. The pictorial representation of the operation is shown in Fig. 11. Let us consider, $m_1 = 2$, and $m_2 = 4$. Therefore, the second and fourth columns are swapped, as shown in Fig. 11.

Algorithm 7 *Verical_Swap*()

$m_1 \leftarrow$ random integer $< Q$
$m_2 \leftarrow$ random integer $< Q$
if $m_1 \neq m_2$ **then**
  Swap m_1^{th} and m_2^{th} columns of C_k
end if

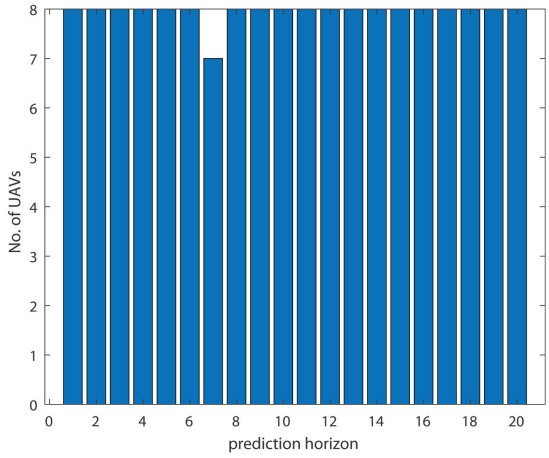


FIGURE 13. The constraints in Eq. 11 is satisfied.

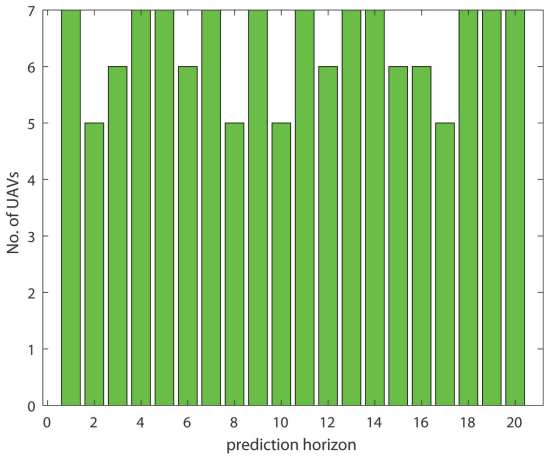


FIGURE 14. The constraints in Eq. 12 is satisfied.

V. SIMULATION RESULTS

In this section simulation results are presented. The simulation scenario consists of 12 aircraft and the prediction horizon is considered as 20. The values of N_L and N_S are selected s 8 and 7 respectively.

The cost J generated by 2D-GA is shown in Fig. 12. The algorithm is allowed to evolve upto fifty generations and it converged in twenty five generations. The solution satisfies the constraints in Eqs. (10-12). The constraints on x (Eq. 11) over the prediction horizon is shown in Fig. 13. It can be observed that the number of aircraft which need to be connected to LOS is less than or equal to N_L at every time instant.The constraints on y (Eq. 12) over the prediction

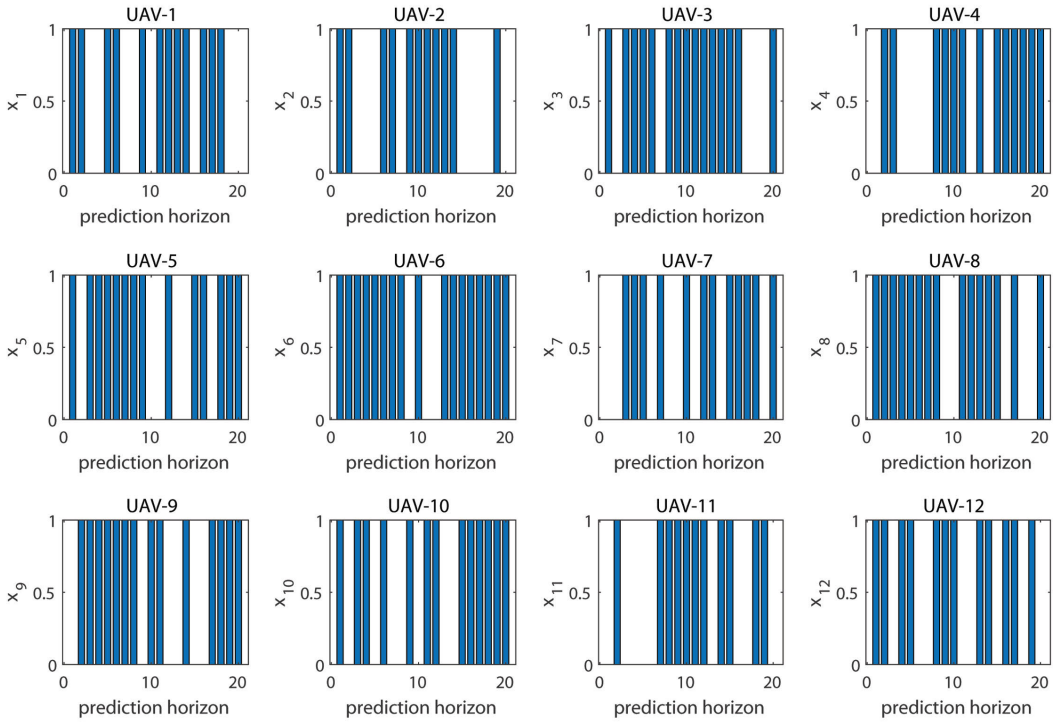


FIGURE 15. Control variable *x* of all aircraft.

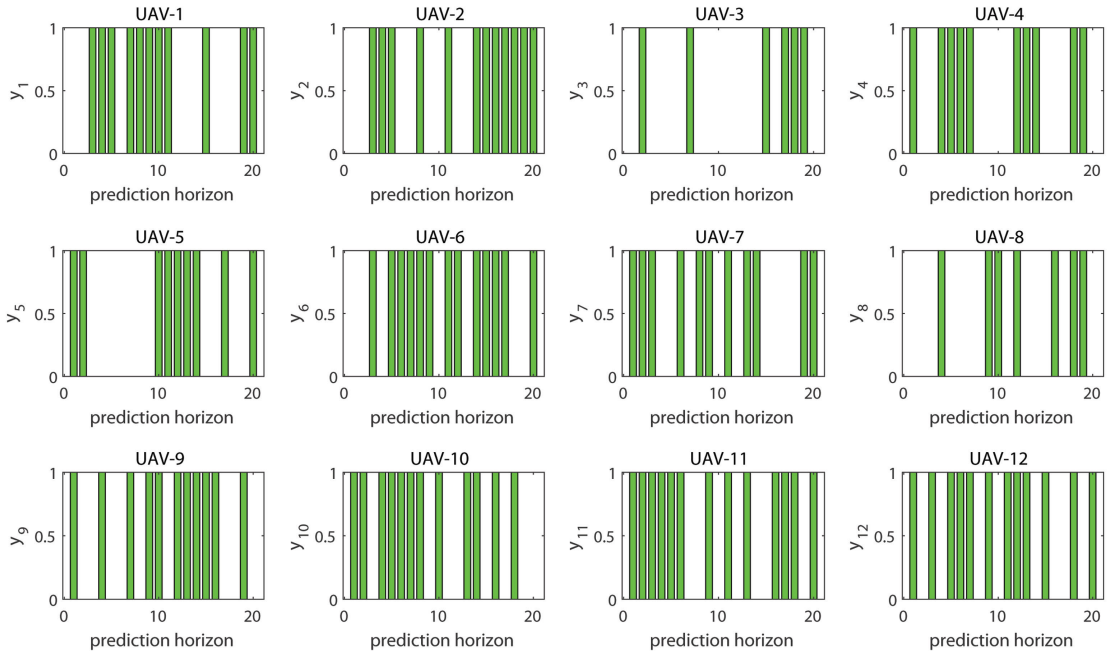


FIGURE 16. Control variable *y* of all aircraft.

horizon is shown in Fig. 14. It can be observed that the number of aircraft which need to be connected to satellite is less than or equal to N_s. The solutions for control variables x_i and y_i $(i = 1, 2, \ldots, 12)$ associated to all the 12 aircraft are shown in Figs. 15 and 16 respectively. The control variables of each aircraft are shown separately. The x and y variables are shown in blue and green colours respectively. The values of the constraints in Eq. 10 are shown in Fig. 17. It can be noticed that the solutions of x and y satisfy the constraint given in Eq. 10, i.e., $x_i(t) + y_i(t) \geq 1$, for each aircraft at each time instant $(k = 1, 2, \ldots, N)$ over the prediction horizon. Therefore, over the prediction horizon, i.e., for the next 20 time instants, we have an optimal solution for handover of dual connectivity.

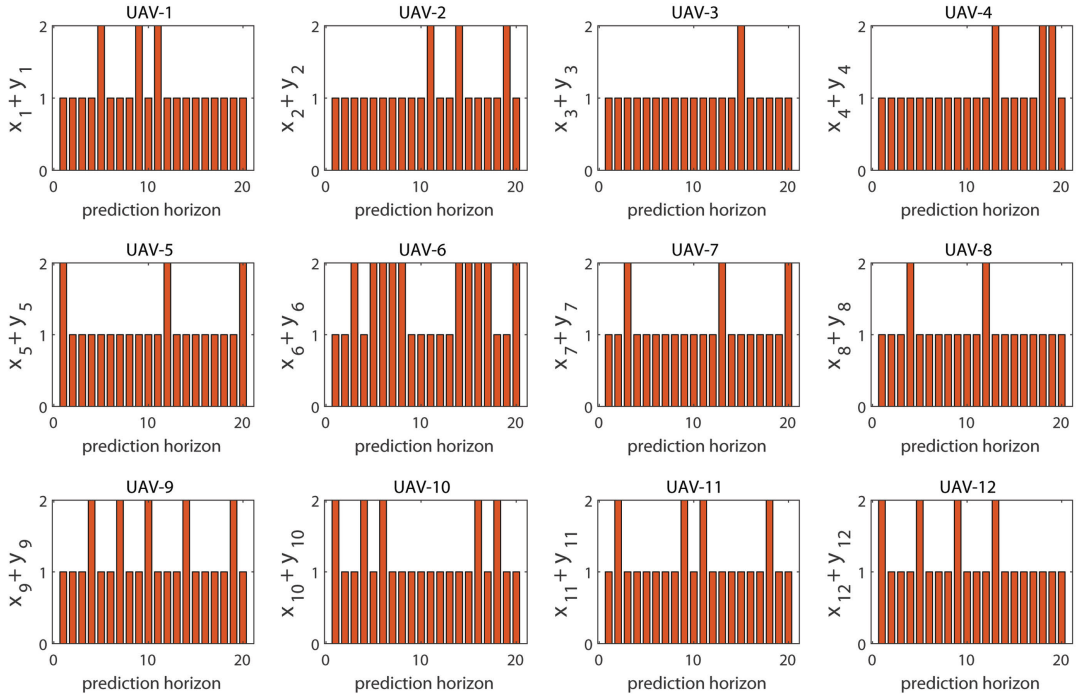


FIGURE 17. Constraint in Eq. 10 is satisfied.

VI. CONCLUSION

The MPC based predictive handover of dual connectivity is a useful mechanism to understand the possible handover between LOS and satellite connection in advance. The formulation resulted in an NLP which can be solved by various available methods. The individual control variables being binary, the use of 2D-GA as a solution method found to be appropriate. The results show that the constraints for each aircraft at each time instant over the prediction horizon are satisfied. The concept may be extremely helpful in case of optimal path planning of UAVs.

REFERENCES

[1] M. Vondra, M. Ozger, D. Schupke, and C. Cavdar, "Integration of satellite and aerial communications for heterogeneous flying vehicles," *IEEE Netw.*, vol. 32, no. 5, pp. 62–69, Sep. 2018.

[2] B. Van Der Bergh, A. Chiumento, and S. Pollin, "LTE in the sky: Trading off propagation benefits with interference costs for aerial nodes," *IEEE Commun. Mag.*, vol. 54, no. 5, pp. 44–50, May 2016.

[3] X. Lin, Z. Zou, V. Yajnanarayana, R. Wiren, S. Euler, A. Sadam, H.-L. Maattanen, S. Muruganathan, S. Gao, Y.-P.-E. Wang, and J. Kauppi, "Mobile network-connected drones: Field trials, simulations, and design insights," *IEEE Veh. Technol. Mag.*, vol. 14, no. 3, pp. 115–125, Sep. 2019.

[4] S. Al-Rubaye and A. Tsourdos, "Airport connectivity optimization for 5G ultra-dense networks," *IEEE Trans. Cognit. Commun. Netw.*, vol. 6, no. 3, pp. 980–989, Sep. 2020.

[5] M. M. Azari, F. Rosas, and S. Pollin, "Cellular connectivity for UAVs: Network modeling, performance analysis, and design guidelines," *IEEE Trans. Wireless Commun.*, vol. 18, no. 7, pp. 3366–3381, Jul. 2019.

[6] L. Yan, X. Fang, and Y. Fang, "A novel network architecture for C/U-plane staggered handover in 5G decoupled heterogeneous railway wireless systems," *IEEE Trans. Intell. Transp. Syst.*, vol. 18, no. 12, pp. 3350–3362, Dec. 2017.

[7] S. Al-Rubaye, A. Al-Dulaimi, J. Cosmas, and A. Anpalagan, "Call admission control for non-standalone 5G ultra-dense networks," *IEEE Commun. Lett.*, vol. 22, no. 5, pp. 1058–1061, May 2018.

[8] C. Rosa, K. Pedersen, H. Wang, P.-H. Michaelsen, S. Barbera, E. Malkamaki, T. Henttonen, and B. Sebire, "Dual connectivity for LTE small cell evolution: Functionality and performance aspects," *IEEE Commun. Mag.*, vol. 54, no. 6, pp. 137–143, Jun. 2016.

[9] D. Wang, Y. Wang, S. Dong, G. Huang, J. Liu, and W. Gao, "Exploiting dual connectivity for handover management in heterogeneous aeronautical network," *IEEE Access*, vol. 7, pp. 62938–62949, 2019.

[10] M. Cannon, "Efficient nonlinear model predictive control algorithms," *Annu. Rev. Control*, vol. 28, no. 2, pp. 229–237, Jan. 2004.

[11] L. Wang, *Model Predictive Control System Design and Implementation Using MATLAB*. London, U.K.: Springer, 2009.

[12] F. Allgöwer and A. Zheng, *Nonlinear Model Predictive Control*, vol. 26. Basel, Switzerland: Birkhäuser, 2012.

[13] H. Chen and F. Allgöwer, "A quasi-infinite horizon nonlinear model predictive control scheme with guaranteed stability," *Automatica*, vol. 34, no. 10, pp. 1205–1217, 1998.

[14] D. Q. Mayne, J. B. Rawlings, C. V. Rao, and P. O. M. Scokaert, "Constrained model predictive control: Stability and optimality," *Automatica*, vol. 36, no. 6, pp. 789–814, Jun. 2000.

[15] S. Jain and H. C. Gea, "Two-dimensional packing problems using genetic algorithms," *Eng. with Comput.*, vol. 14, no. 3, pp. 206–213, Sep. 1998.

[16] M.-W. Tsai, T.-P. Hong, and W.-T. Lin, "A two-dimensional genetic algorithm and its application to aircraft scheduling problem," *Math. Problems Eng.*, vol. 2015, Mar. 2015, Art. no. 906305.

[17] S. Mondal and A. Tsourdos, "Optimal topology for consensus using genetic algorithm," *Neurocomputing*, vol. 404, pp. 41–49, Sep. 2020.

[18] S. Mondal and A. Tsourdos, "Autonomous addition of agents to an existing group using genetic algorithm," *Sensors*, vol. 20, no. 23, p. 6953, Dec. 2020.

[19] K. A. De Jong and W. M. Spears, "A formal analysis of the role of multi-point crossover in genetic algorithms," *Ann. Math. Artif. Intell.*, vol. 5, no. 1, pp. 1–26, Mar. 1992.

[20] G. Syswerda, "Uniform crossover in genetic algorithms," in *Proc. 3rd Int. Conf. Genetic Algorithms*. Burlington, MA, USA: Morgan Kaufmann, 1989, pp. 2–9.

[21] L. B. Booker, D. E. Goldberg, and J. H. Holland, "Classifier systems and genetic algorithms," *Artif. Intell.*, vol. 40, nos. 1–3, pp. 235–282, Sep. 1989.

[22] P. Kora and P. Yadlapalli, "Crossover operators in genetic algorithms: 1 A review," *Int. J. Comput. Appl.*, vol. 162, no. 10, pp. 34–36, Mar. 2017.



https://dspace.org/

Handover prediction for aircraft dual connectivity using model predictive control

Mondal, Sabyasachi; Al-Rubaye, Saba; Tsourdos, Antonios

2021-03-17
IEEE
https://doi.org/10.1109/ACCESS.2021.3066554
Mondal S, Al-Rubaye S, Tsourdos A. (2021) Handover prediction for aircraft dual connectivity using model predictive control. IEEE Access, Volume 9, 2021, pp. 44463-44475

Downloaded from a DSpace repository. https://dspace.org/